Sensors and Materials, Vol. 34, No. 4 (2022) 1577–1586
MYU Tokyo

S & M 2911

Performance Comparison between Atomic-layer-deposited Al_2O_3/HfO_2 Nanolaminate and Parylene C for Implantable Devices with High Step Coverage Using Accelerated Life Testing

Takuro Kono,[1] Yasuo Terasawa,[1*] Hiroyuki Tashiro,[2,3] Tokio Ueno,[1] and Jun Ohta[2]

[1]Artificial Vision Institute, R&D Div., Nidek Co., Ltd., 13-2 Hama-cho, Gamagori, Aichi 443-0036, Japan
[2]Materials Science, Nara Institute of Science and Technology, 8916-5 Takaya-cho, Ikoma, Nara 630-0192, Japan
[3]Division of Medical Technology, Department of Health Sciences, Faculty of Medical Sciences, Kyushu University, 3-1-1 Maidashi, Higashi-ku, Fukuoka 812-8582, Japan

(Received November 5, 2021; accepted March 14, 2022)

Keywords: hermetic packaging, Al_2O_3/HfO_2 nanolaminate, long-term reliability, wireless measurement system

Hermetic packaging with biocompatibility and long-term reliability is essential for implantable devices. Parylene C is widely used because of its high biocompatibility, low dielectric constant, and resistance to moisture permeation. However, it degrades during long-term use and has limited step coverage. A film deposited by atomic layer deposition (ALD) is an alternative to Parylene C. The self-limiting reaction of the ALD process results in the formation of a thin conformal layer with high step coverage and low pinhole density. Also, reliability evaluation has been performed on samples with low step coverage, such as thin-film metal patterns. In this study, to evaluate the reliability of high-step-coverage samples, an Al_2O_3/HfO_2 nanolaminate was deposited by ALD on high-step-coverage samples with a coil element connected to a thin-film capacitor, and accelerated tests were conducted in phosphate-buffered saline at 77 °C. In addition, the insulating property of the packaging was evaluated by the capacitor impedance at a frequency with an impedance phase angle, which was detected wirelessly by coupling between the sample and measurement coils. Our findings demonstrate that the Al_2O_3/HfO_2 nanolaminate functions as an effective barrier at 77 °C for 83 days. However, following accelerated tests, cracks in the Al_2O_3/HfO_2 nanolaminate were found at coil connection sites. These results suggest that ALD has utility in various geometries for the packaging of implantable devices; however, modified connection configurations are necessary.

1. Introduction

The stability of operation in implantable devices is highly dependent on the performance of hermetic packaging. In the past, hard and heavy metal cases, such as titanium (Ti) cases, were used for packaging.(1) However, a hermetic packaging made of a polymer material has recently

*Corresponding author: e-mail: yasuo_terasawa@nidek.co.jp
https://doi.org/10.18494/SAM3727

ISSN 0914-4935 © MYU K.K.
https://myukk.org/

been used owing to the miniaturization of implant devices.[2,3] Parylene C is a typical example of a hermetic packaging made of a polymer material. Parylene C has USP Class VI biocompatibility, low water permeability, and excellent insulating properties, and can be deposited at room temperature.[4,5] However, the barrier property of Parylene C deteriorates significantly during long-term use owing to cracking, delamination, and erosion.[6] For this reason, films deposited by atomic layer deposition (ALD) are attracting attention as a packaging that can withstand long-term use.

The self-limiting reaction of the ALD process results in the formation of a thin conformal layer with high step coverage and low pinhole density.[7,8] This layer is also known to exhibit good insulating properties and low water permeability.[9–11] The functionality and durability of ALD films have been confirmed by accelerated degradation tests and have been shown to be superior to those of Parylene C.[12] Moreover, the reliability of ALD can be improved by layering different film types.[13] Leakage current measurement[14] and the calcium (Ca) conductance test[15] are widely used for reliability evaluation. Such evaluation has been performed on samples with low step coverage, such as thin-film metal patterns. However, an implantable device with a custom integrated circuit (IC) implemented[16] has a higher aspect ratio than a sample used for reliability evaluation. Therefore, testing with high-step-coverage samples is more appropriate for observing the performance of packaging for implantable devices.

In this study, to implement ALD in implantable devices, the reliability of ALD for samples with high step coverage was evaluated in accelerated life testing in comparison with that of Parylene C. Al_2O_3,[8] which has high adhesion to the substrate and good barrier properties against water and ions, and HfO_2,[17] which is stable in biological environments, were selected for ALD.

2. Materials and Methods

2.1 Measurement system setup

To avoid artifact damage to the sample, the insulation properties of the packaging were measured using a wireless measurement system with a receiver coil connected to the sample and coupled to a measurement coil. The measurement system is shown in Fig. 1(a). Measurements were taken with the distance between coils fixed at 2 mm using a fixture. A ferrite rod that protruded 3.5 mm from the measuring coil was fixed, and the protruding part was inserted into the receiving coil. This allowed the ferrite rod to straddle both coils. In this experiment, the measurement and receiver coils were immersed in phosphate-buffered saline (PBS) to stabilize the measurement. Figure 1(b) shows a schematic image of the measurement environment and a cross-sectional view of the positional relationship between the measurement and receiver coils.

2.2 Fabrication of high-step-coverage device

A 20 nm Ti layer and a 200 nm gold (Au) layer were deposited on glass by radio frequency sputtering. Contact photolithography was used to create patterned thin-film capacitors, followed by the wet etching of Ti and Au. A receiver coil (760308101216, 1.5 mm thickness, 6 mm

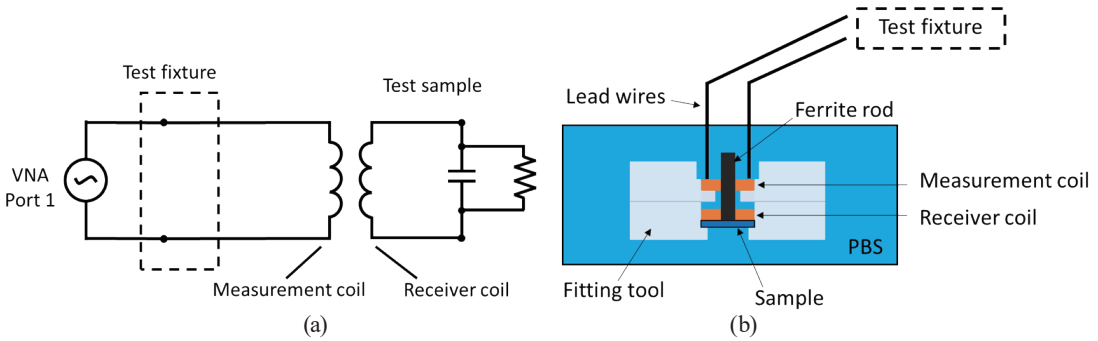

Fig. 1. (Color online) (a) Setup of the wireless measurement system. (b) Schematic of accelerated life testing setup. VNA: vector network analyzer. PBS: phosphate-buffered saline.

diameter, Wurth Elektronik) was connected to the fabricated thin-film capacitor pattern using a conductive adhesive containing a silver filler (CR-2800, KAKEN TECH Co., Ltd.).

ALD was performed by Picosun Japan Co., Ltd. The ALD nanolaminate was deposited in an R-200 Advanced ALD tool (Picosun, Finland) by thermal ALD at 150 °C. Alternating layers of a HfO_2-based ALD nanolaminate were deposited with a total film thickness of 100 nm. The thickness of the ALD nanolaminate deposited on a silicon wafer was measured using an ellipsometer (SE2000, Semilab).

Parylene C was deposited to the specified film thickness using a lab coater (PDS-2010, SCS) (Table 1). The thickness of Parylene C deposited on a glass substrate was measured with a white interference microscope (Profilm3D, Filmetrics).

For the measurement coil, a ferrite rod (3078990901, Fair-Rite) was polished and connected to the coil (760308101216, 1.5 mm thickness, 6 mm diameter, Wurth Elektronik). The measurement coil was soldered and fixed to the universal board. The connection of the measurement coil was sealed with silicone (MED4211, Nusil), and the entire measurement coil was coated with a 5-mm-thick film of Parylene C.

2.3 Accelerated life testing

To mimic the environment of extracellular tissues, the samples were fixed in a fixture and immersed in 0.01 mol/L PBS (pH 7.2–7.4) at 77 °C. The continuous operating temperature of Parylene C was 80 °C. The experimental temperature T was set to 77 °C, which gave the largest integer of the acceleration factor when the body temperature T_{nat} was 37 °C. The samples were tested in separate containers for each film type and thickness. The acceleration factor was calculated using the Arrhenius equation with Eq. (1).[18] The acceleration factor was 16.

$$\begin{aligned} &Accelerated\ aging\ by\ factor = f \\ &f = 2^{\Delta T/10} \\ &\Delta T = T - T_{nat} \end{aligned} \tag{1}$$

The testing period was set at 228 days to demonstrate durability for 10 years *in vivo*. The

Table 1
Thickness of each material and number of samples.

Material	Thickness (μm)	Number of samples
Al_2O_3/HfO_2	0.11	10
Parylene C	0.12	4
	4	6

measurement of each sample was terminated when the insulation of the packaging was lost. The accelerated life testing was terminated when all the samples had broken. The measurement was continued regardless of the insulation of the package for up to 23 days (equivalent to 1 year). After the accelerated life testing, the surface was observed by scanning electron microscopy.

2.4 Measurement of insulation characteristics

The insulation characteristics of the packaging are defined by the resistance R and capacitor C of the parallel RLC circuit, and their changes can be evaluated by wireless measurement.[19] In previous studies, an oscilloscope and a function generator were used to measure the quality factor. In this study, the measurement system was replaced by a network analyzer (E5061B, Keysight). The test system was made equivalent by measuring S_{11} of one port. To directly record the changes in insulation characteristics, Z was calculated from Eq. (2).

$$\begin{aligned} &\textit{Reference impedance} = Z_0 \\ &Z = Z_0 \frac{1+S_{11}}{1-S_{11}} \end{aligned} \tag{2}$$

The phase angle of the resistance was concurrently measured, and the peak value was calculated from each frequency characteristic. The temperature was returned to room temperature during the measurement. The destruction of the packaging was defined as a change in capacitance accompanied by a decrease in synthetic resistance and a change in relative permittivity. The insulation characteristics of the film were evaluated from the phase angle peak of the synthetic resistance of the sample at each frequency. If the packaging is degraded, the synthetic resistance will decrease. At the same time, the capacitance of the sample capacitor will increase with the relative dielectric constant of the insulator. The phase angle peak at each frequency shifts from the initial position to the lower frequency side. When the insulation performance is lost, the phase angle peak is lost.

The lifetime of the samples was determined by plotting the survival probability using the Weibull distribution and calculating the median time to fail (MTTF). Software (Kyplot v.6.0, KyensLab Inc.) was used to calculate the MTTF.

3. Results and Discussion

3.1 Analysis of phase angle at each frequency under accelerated life testing

An LC circuit was fabricated on a glass substrate for the measurement sample [Fig. 2(a)]. The capacitor section has a capacitance of 9.1 pF in the undeposited state [Fig. 2(b)]. A typical example of the phase angle and impedance at each frequency is shown in Fig. 3. The self-

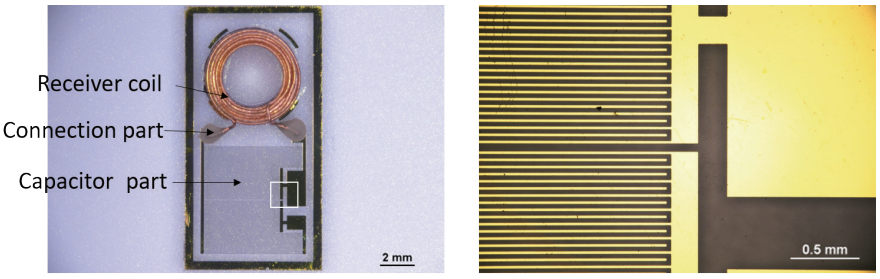

(a) (b)

Fig. 2. (Color online) (a) High-step-coverage sample. (b) High-magnification image of the white square.

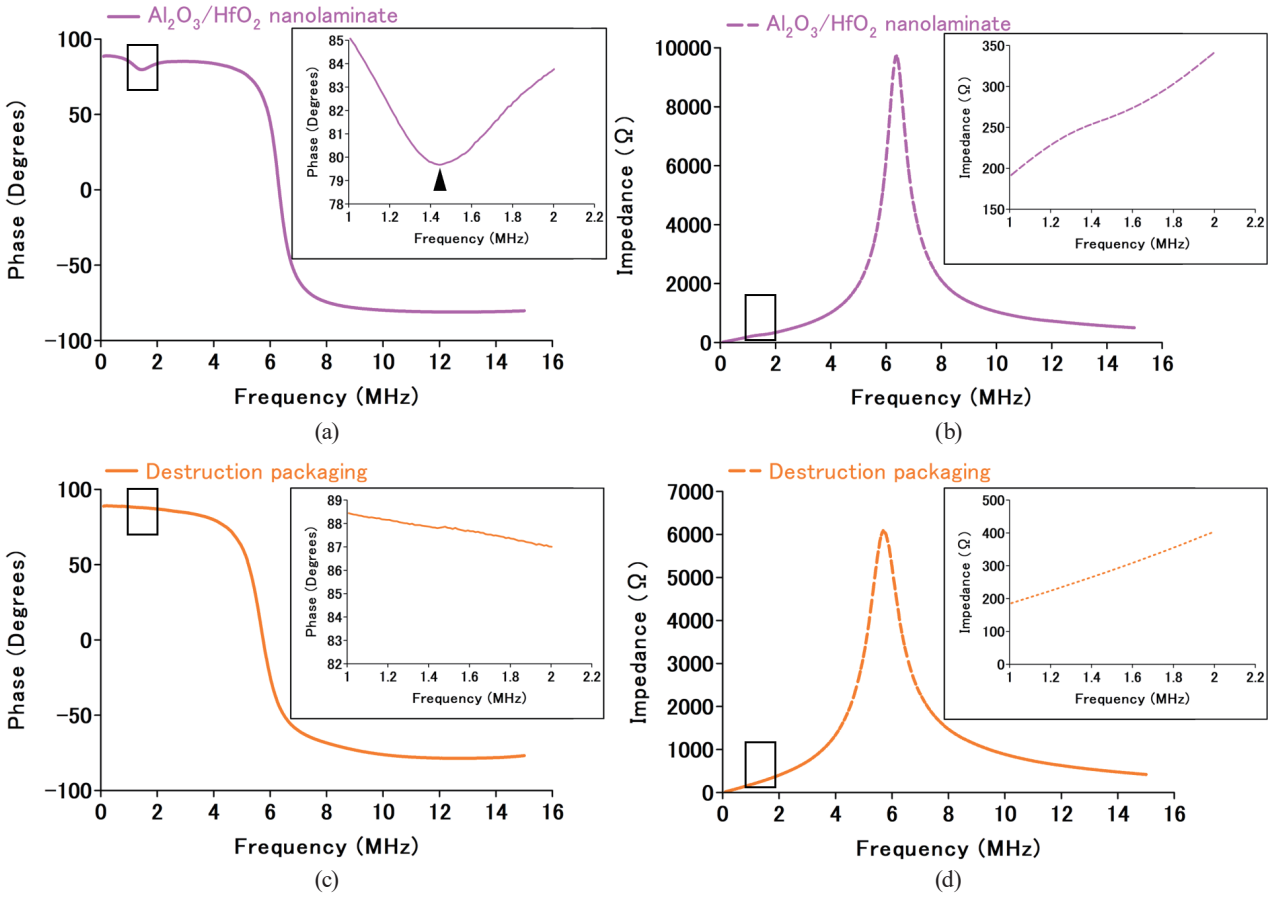

(a) (b) (c) (d)

Fig. 3. (Color online) Typical example of the phase angle and impedance at each frequency. The inset shows an enlarged graph of the 1–2 MHz bands. Arrowhead: peak of phase angle.

resonant frequency of the measurement coil was 6 MHz, and the resonant frequency with the receiver coil appears as a phase angle peak. The Al_2O_3/HfO_2 nanolaminate sample exhibited a characteristic peak of the phase angle at around 1.4 MHz [Fig. 3(a)]. In contrast, the peak is not visible for the sample simulating a broken condition, where the film was removed from the capacitor section of the Parylene C sample to enable the evaluation of the capacitor section only [Fig. 3(c)]. In the same way, the Parylene C samples showed peaks at around 2.6 MHz at 0.12 μm [Fig. 4(a)] and 8 MHz at 4 μm [Fig. 4(b)]. The direction of the phase angle change is opposite for Figs. 4(a) and 4(b) because the frequency properties (inductive or capacitive) were reversed at around 6 MHz. The impedance peaks at frequencies where phase angle peaks were identified are indistinct [Fig. 3(b)]. Therefore, the reliability of the packaging was evaluated by comparing the phase angle peak differences obtained before and after testing.

The number of surviving samples during the accelerated life testing period is shown in Fig. 5. The Al_2O_3/HfO_2 nanolaminate samples were broken over time, and all samples were broken on

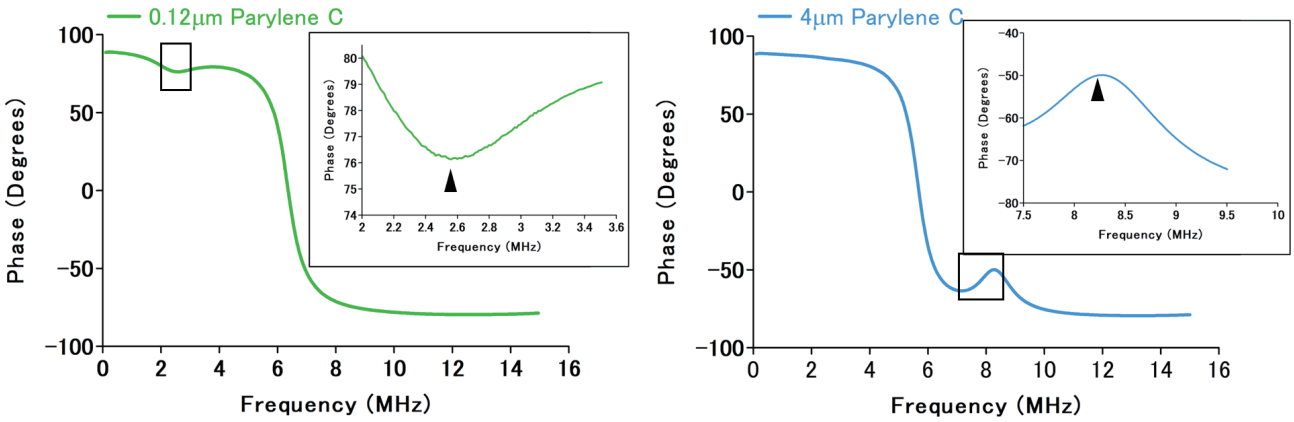

(a) (b)

Fig. 4. (Color online) Typical example of phase angle at each frequency for each thickness of Parylene C. The inset shows an enlarged graph of the area near the phase angle peak. Arrowhead: peak of phase angle.

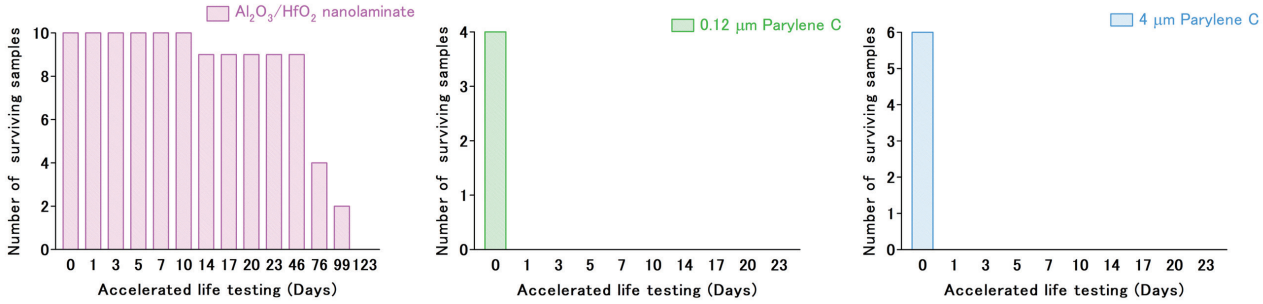

(a) (b) (c)

Fig. 5. (Color online) Number of surviving samples during the accelerated life testing period. (a) Al_2O_3/HfO_2 nanolaminate samples ($N = 10$). (b) 0.12 mm Parylene C samples ($N = 4$). (c) 4 mm Parylene C samples ($N = 6$). N is the number of tested samples.

day 123 [Fig. 5(a)]. The results for the Al_2O_3/HfO_2 nanolaminate samples are shown as survival probabilities in the form of a Weibull distribution in Fig. 6. The shape parameter of the Weibull distribution was estimated to be 3.14 and the scale parameter (η) was estimated to be 92.70. The MTTF of the Al_2O_3/HfO_2 nanolaminate sample was 83 days in PBS at 77 °C, which corresponds to 1328 days at 37 °C. Alternatively, the measured phase of the Parylene C samples exhibited a change on the first day of testing [Figs. 5(b) and 5(c)]. These results show that the Al_2O_3/HfO_2 nanolaminate is superior to Parylene C in terms of the reliability of the hermetic packaging for the high-step-coverage samples. Parylene C lost its hermeticity in a day, a possible explanation of which is the change in the resistance of the film due to swelling. Parylene C has been shown to decrease in resistance in a short time when immersed in PBS.[5] In addition, since no pre-treatment such as with a silane coupling agent was used to improve adhesion, a possible explanation of which is that PBS will penetrate between Parylene C and the sample if there is a pinhole. Since the peak frequency of the phase angle depends on the resistance of the sample (Figs. 3 and 4), we conclude that it can reflect the change in resistance that precedes the breakdown of the film.

3.2 Observation of Al_2O_3/HfO_2 nanolaminate after accelerated life testing

The degradation of thin-film packaging during long-term use includes the physical breakdown and chemical change of the film. Therefore, the surface condition of the Al_2O_3/HfO_2 nanolaminate sample at 77 °C after 123 days was observed using a scanning electron microscope. A significant crack at the connection with the coil was observed (Fig. 7). However, no significant cracks were observed in the capacitor part. The result shows that one of the causes of the hermeticity breakdown of the Al_2O_3/HfO_2 nanolaminate is the formation of cracks in the conductive resin employed for the connection between the coil and the comb-pattern-formed glass substrate. In conclusion, the difference in the coefficient of thermal expansion of the

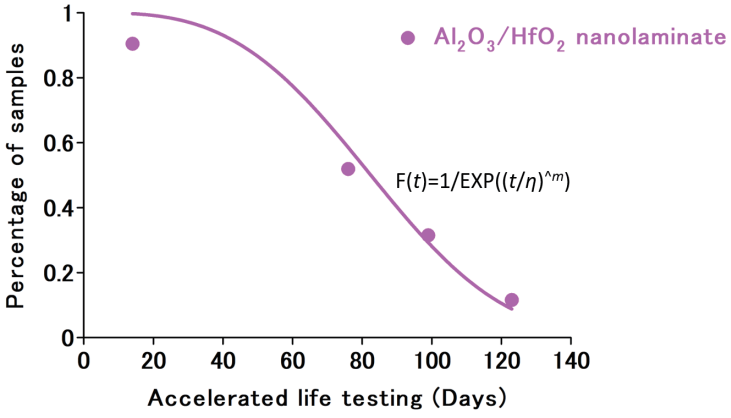

Fig. 6. (Color online) Survival rate of Al_2O_3/HfO_2 nanolaminate samples. t: accelerated life testing time, η: scale parameter, and m: shape parameter.

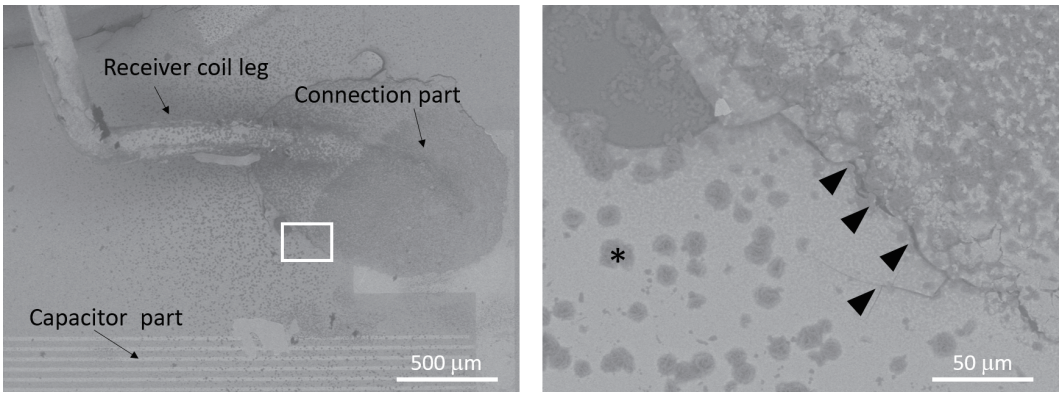

(a) (b)

Fig. 7. (a) SEM image of the coil connection after the accelerated life testing. (b) High-magnification image of the white square in (a). Arrowheads: cracks in the Al_2O_3/HfO_2 nanolaminate. Asterisk: deposits of Ag.

materials caused the Al_2O_3/HfO_2 nanolaminate to crack in the bonding area. The coefficient of thermal expansion of the ALD film is 5–7 ppm/K,[20] that of glass is 3.25 ppm/K,[21] that of conductive resin epoxy resin is 47.5 ppm/K,[22] and that of the silver filler agent is typically 19 ppm/K.[23] Under accelerated testing conditions, the epoxy resin expands and stresses the ALD film.

4. Conclusion

The phase angle at each frequency was evaluated under accelerated testing conditions to observe the packaging performance of an Al_2O_3/HfO_2 nanolaminate with high step coverage for implant devices. The Al_2O_3/HfO_2 nanolaminate showed reliability for about 4 years in PBS at 37 °C, indicating that it was more effective than Parylene C as a packaging material. However, this is still less than the recommended lifetime of an implant device of at least 5 years.[24]

One of the causes of ALD film destruction was a crack in the resin material used to connect the coil because no sudden changes in electrical properties due to swelling originating from the environment of extracellular tissues were observed in the ALD film. In conclusion, cracks were caused by a mismatch of the coefficient of thermal expansion in the material composition. The cracks caused by this mismatch were mainly due to the accelerated life testing conditions. However, in practical uses, such as product manufacturing, transportation, and sterilization, heat stress is expected. Because an ALD film is almost incapable of being deformed, ALD is not a suitable method for depositing a top layer on an easily deformable resin. The use of conductive adhesives rather than resin materials for the connection could prevent deterioration caused by the coefficient of thermal expansion mismatch. Metal bonding is an efficient choice for mounting elements. Moreover, by depositing an ALD layer in the resinous encapsulating material, i.e., forming a resin–ALD layer–resin structure, it is possible to provide durability against fracture caused by the coefficient of thermal expansion mismatch.[13] A resin–ALD–resin structure

shows a higher long-term reliability than the resin alone,[13] allowing the size of the package to be reduced.

ALD membranes can be used as long-term hermetic packaging for high-aspect-ratio implantable devices by adopting a mounting configuration that reduces the difference in thermal expansion coefficient among the materials. Therefore, two strategies are being considered for future studies. The first strategy is to fabricate and evaluate samples using a bonding method that does not require resin for connection, such as ultrasonic bonding. The other is to study the conditions required for achieving both deformation-following and barrier properties by adjusting the thickness of the laminate film of the resin and ALD film. Thus, the above-mentioned strategies are expected to produce implantable devices with a guaranteed *in vivo* reliability of 10 years or more.

Acknowledgments

The research on ALD was supported by Picosun Japan Co., Ltd.

Conflicts of interest

Takuro Kono, Yasuo Terasawa, and Tokio Ueno are employees of Nidek Co., Ltd. Hiroyuki Tashiro and Jun Ohta received a research grant from Nidek Co., Ltd.

References

1. M. Birkholz, P. Glogener, F. Glös, T. Basmer, and L. Theuer: Micromachines **7** (2016) 183. https://doi.org/10.3390/mi7100183
2 K. Scholten and E. Meng: Lab. Chip. **15** (2015) 4256. https://doi.org/10.1039/C5LC00809C
3 S. P. Lacour, G. Courtine, and J. Guck: Nat. Rev. Mater. **1** (2016) 16063. https://doi.org/10.1038/natrevmats.2016.63
4 D. C. Rodger, A. J. Fong, W. Li, H. Ameri, I. Lavrov, H. Zhong, S. Saati, P. Menon, E. Meng, J. W. Burdick, R. R. Roy, V. R. Edgerton, J. D. Weiland, M. S. Humayun, and Y. C. Tai: Conf. IEEE, Lyon, France (2007) 1385 https://doi.org/10.1109/SENSOR.2007.4300401
5 J. P. Seymour, Y. M. Elkasabi, H.-Y. Chen, J. Lahann, and D. R. Kipke: Biomaterials **30** (2009) 6158. https://doi.org/10.1016/j.biomaterials.2009.07.061
6 X. Xie, L. Rieth, R. Caldwell, M. Diwekar, P. Tathireddy, R. Sharma, and F. Solzbacher: IEEE Trans. Biomed. Eng. **60** (2013) 2943. https://doi.org/10.1109/TBME.2013.2266542
7 S. M. George: Atomic Layer Deposition: Chem. Rev. **110** (2010) 111. https://doi.org/10.1021/cr900056b
8 H. Wang, Y. Liu, H. Liu, Z. Chen, P. Xiong, X. Xu, F. Chen, K. Li, and Y. Duan: Adv. Mater. Interfaces **5** (2018) 1701248. https://doi.org/10.1002/admi.201701248
9 K. H. Yoon, H. S. Kim, K. S. Han, S. H. Kim, Y. E. K. Lee, N. K. Shrestha, S. Y. Song, and M. M. Sung: ACS Appl. Mater. Interfaces, **9** (2017) 5399. https://doi.org/10.1021/acsami.6b15404
10 H. Zhang, H. Ding, M. Wei, C. Li, B. Wei, and J. Zhang: Nanoscale Res. Lett. **10** (2015) 169. https://doi.org/10.1186/s11671-015-0857-8
11 E. Langereis, M. Creatore, S. B. S. Heil, M. C. M. van de Sanden, and W. M. M. Kessels: Appl. Phys. Lett. **89** (2006) 081915. https://doi.org/10.1063/1.2338776
12 S. Minnikanti, G. Diao, J. J. Pancrazio, X. Xie, L. Rieth, F. Solzbacher, and N. Peixoto: Acta Biomater. **10** (2014) 960. https://doi.org/10.1016/j.actbio.2013.10.031
13 C. Li, M. Cauwe, L. Mader, D. Schaubroeck, and M. Op de Beeck: Coatings **10** (2019) 19. https://doi.org/10.3390/coatings10010019
14 J. Jeong, F. Laiwalla, J. Lee, R. Ritasalo, M. Pudas, L. Larson, V. Leung, and A. Nurmikko: Adv. Funct. Mater. **29** (2019) 1806440. https://doi.org/10.1002/adfm.201806440

15 K. H. Yoon, H. Kim, Y.-E. Koo Lee, N. K. Shrestha, and M. M. Sung: RSC Adv. **7** (2017) 5601. https://doi.org/10.1039/C6RA27759D
16 Y. Terasawa, A. Uehara, E. Yonezawa, T. Saitoh, K. Shodo, M. Ozawa, Y. Tano, and J. Ohta: IEICE Electron. Express **5** (2008) 574. https://doi.org/10.1587/elex.5.574
17 J. M. H. Morales, C. Gaude, D. Ratel, J.-C. Souriau, G. Simon, and F. Berger: Proc. World Congress on Electrical Engineering and Computer Systems and Science (EECSS, 2015) 322.
18 General Aging Theory and Simplified Protocol for Accelerated Aging of Medical Devices: https://www.mddionline.com/design-engineering/general-aging-theory-and-simplified-protocol-accelerated-aging-medical-devices?_sp=70e6e4f1-0455-4490-b637-560a70b71e66.1645495498350 (accessed February 2022).
19 X. Huang, P. M. Denprasert, L. Zhou, A. N. Vest, S. Kohan, and G. E. Loeb: Biomed. Microdevices **19** (2017) 46. https://doi.org/10.1007/s10544-017-0189-9
20 D. C. Miller, R. R. Foster, S. -H. Jen, J. A. Bertrand, S. J. Cunningham, A. S. Morris, Y. -C. Lee, S. M. George, and M. L. Dunn: Sens. Actuators, A **164** (2010) 58. https://doi.org/10.1016/j.sna.2010.09.018
21 N. Bouras, M. A. Madjoubi, M. Kolli, S. Benterki, and M. Hamidouche: Phys. Procedia **2** (2009) 1135. https://doi.org/10.1016/j.phpro.2009.11.074
22 E. Foo, M. Jaafar, A. Aziz, and L. C. Sim: Compos. Part Appl. Sci. Manuf. **42** (2011) 1432. https://doi.org/10.1016/j.compositesa.2011.06.007
23 K. Asaoka and N. Kuwayama: Dent. Mater. J. **9** (1990) 47123. https://doi.org/10.4012/dmj.9.47
24 Investigational Device Exemption (IDE) Guidance for Retinal Prostheses: https://www.fda.gov/regulatory-information/search-fda-guidance-documents/investigational-device-exemption-ide-guidance-retinal-prostheses (accessed October 2021).